International Journal of Research
Available at https://edupediapublications.org/journals
e-ISSN: 2348-6848
p-ISSN: 2348-795X
Volume 04 Issue-17
December 2017

Reactive Power Disturbance with an Islanding Detection Method for Inverter-Based Distributed Generators Using Fuzzy Controller

Md.Ather Ali & K.Rama Krishna
[1]M.Tech, B.V.Raju Institute of Technology, Narsapur, Telangana, India..
[2]Associate Professor, B.V.Raju Institute of Technology, Narsapur, Telangana, India.

.

Abstract-*An fuzzy control based islanding detection technique for distributed generators are proposed in this paper by using of MATLAB/SIMULINK. The islanding detection technique for inverter-based distributed generators (DGs) is exhibited, which depends on annoying receptive power yield. In this paper, we are using the fuzzy controller compared to other controllers. Fuzzy controller is denoted as human decision making mechanism which provided the operation for the electronic system with the expert decision. Two arrangements of unsettling influences are designed in this technique, which have distinctive amplitudes and span time. The first arrangement describes the set of reactive power disturbance (FSORPD) is occasional with amplitudes to break the receptive power adjust amid islanding, while the greatness of the second set of reactive power disturbance (SSORPD) is adequate to drive the recurrence to stray outside its edge limits. Considering all the conceivable recurrence variety qualities with the FSORPD subsequent to islanding, three paradigms are intended for changing the unsettling influence from the FSORPD to the SSORPD. In this manner, synchronization of the SSORPDs can be ensured for the framework with numerous DGs and the strategy can identify islanding with a zero non location zone property. Besides, the technique can be connected to the DG either working at solidarity control factor or providing receptive power to for its nearby load.*

Index Terms—Disturbance synchronization, inverter-based distributed generation, islanding detection, reactive power disturbance, fuzzy control.

I. INTRODUCTION

This paper is deal about the Islanding which have the condition in which a portion of the utility system can consist of both the DG and load along with the continues operating during this portion is electrically which is separated from the main utility. Islanding can be result in power quality problems, serious equipment damage, and even safety hazards to utility operation personnel and many more. Therefore the maximum delay may be 2 s which is required for the detection of an islanding and a generic system for islanding detection study is recommended as well, where the distributed network, the RLC load and the DG are connected at the point of common coupling (PCC).

Islanding detection methods are divided into following three categories: 1) active methods; 2) communication-based methods; and3) passive methods. Therefore the communication based methods may not have the harmful effect to the power quality of the power system and it may not have the non detection zones (NDZs) in the theory. However, the cost is much increase because of the need of communication infrastructure and the operations are more complex as well.

Therefore to decrease or eliminate the NDZ, active methods rely on intentionally injecting disturbances, negative sequence components or harmonics into some DG parameters to identify whether islanding has occurred. Though active methods suffer smaller NDZs, they sacrifice power quality and reliability of the power system during normal operation. Moreover, some active methods have difficulty in maintaining synchronization of the intentional disturbances. Therefore, they may not work owing to the averaging effect when applied in multiple-DG operation.

The main aim of this paper is too inspired for the studies. So the main objective is an islanding detection method which is depends upon the intermittent bilateral reactive power variation (RPV) which has been proposed. Therefore the variation in the amplitude is about 5% of the DG's active power output. The frequency was eventually forced to deviate outside the normal range during islanding due to the reactive power variation. When Compared with the method and the method proposed and it was improved by only outputting unilateral RPV in each variation period and further reducing the variation amplitude based on the load's resonance frequency detection.

The proposed method has following three distinguishing features: 1) It can be applied to the DG either operating at unity power factor or supplying reactive power as well for its local load; 2) Synchronization of the disturbances can be guaranteed for the system with multiple DGs and the method can detect islanding with the zero NDZ

International Journal of Research
Available at https://edupediapublications.org/journals
e-ISSN: 2348-6848
p-ISSN: 2348-795X
Volume 04 Issue-17
December 2017

property; 3) The perturbation of reactive power is further reduced during normal operation.

II. BASIC RELATIONSHIP ANALYSIS AND RPV METHODS

A. System Modeling and Basic Relationship Analysis

According to the recommended test system for islanding detection study is shown in Fig. 1. As shown in Fig. 1(a), when the DG is connected to the utility grid, the following equations describe the power flows and the active and reactive power consumed by the load:

$$P_{Load} = P_{DG} + P_{Grid} = 3\frac{V_{PCC}^2}{R} \quad (1)$$

$$Q_{Load} = Q_{DG} + Q_{Grid} = 3V_{PCC}^2\left(\frac{1}{2\pi fL} - 2\pi fC\right) \quad (2)$$

Where VPCC and f are the phase voltage at the PCC and its frequency, and R, L, C represents the load resistance, inductance, and capacitance, respectively.

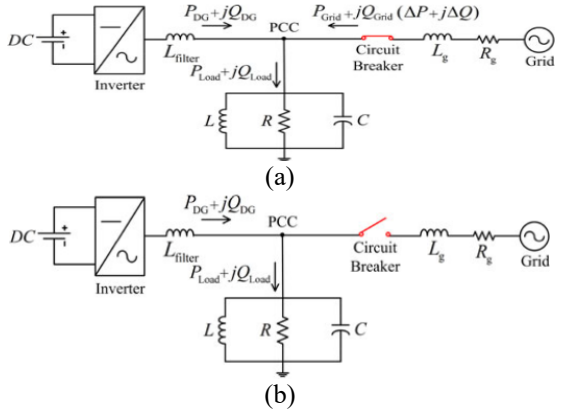

Fig. 1. Test system for islanding detection study (a) Grid-connected operation mode (b) Islanding operation mode

It consists of an inverter-based DG, a parallel RLC load and the grid represented by a source behind impedance. The operation mode of the DG depends on whether the circuit breaker is closed or not

Fig. 2 presents the block diagram of the DG interface control. The phase-locked loop (PLL), the outer power control loop and the inner current control loop are three main parts

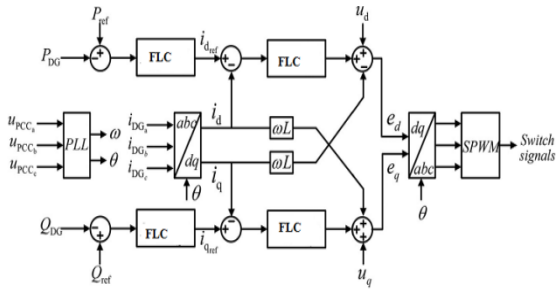

Fig. 2. DG interface control for constant power operation.

Moreover, the load's resonant Frequency ($f0$) and quality factor (If) can be expressed as

$$Q_f = R\sqrt{\frac{C}{L}} = 2\pi f_o RC \quad (3)$$

$$f_o = \frac{1}{2\pi\sqrt{LC}} \quad (4)$$

According to IEEE Std.929, Qf is typically set at 2.5. By combining (1), (3), and (4), (2) can be rewritten as follows:

$$Q_{Load} = P_{Load}\, Q_f\left(\frac{f_o}{f} - \frac{f}{f_o}\right) \quad (5)$$

On the other hand, when islanding occurs as shown in Fig. 1(b), it can be inferred from (1) that if the active power mismatch ΔP(ΔP = PLoad − PDG = PGrid) is not equal to zero, the PCC voltage will fall or rise no matter the DG operates at unity power factor or not. The amount of voltage deviation depends on the value of ΔP. If the active power reference of the DG is set to be constant, ΔP can be expressed as follows.

$$\Delta P = P_{DG}\left(\frac{1}{(1+\Delta V)^2} - 1\right) \quad (6)$$

Where ΔV represents the voltage deviation and it can be expressed as

$$\Delta V = \frac{V_{PCC.i} - V_{PCC}}{V_{PCC}} \quad (7)$$

Where VPCC and VPCC.i represent the PCC voltage before and after islanding, respectively. If the active power mismatch is not large enough, the passive OVP/UVP method will suffer the NDZ due to inadequate changes of the PCC voltage. Thus, the frequency variation also can be used to detect islanding based on the OFP/UFP method.

According to (5), the load's reactive power consumption after islanding (QLoad.i) can be expressed as follows:

$$Q_{Load.i} = Q_{DG} = P_{Load.i} Q_f\left(\frac{f_o}{f_i} - \frac{f_i}{f_o}\right)$$

$$= P_{DG} Q_f\left(\frac{f_o}{f_i} - \frac{f_i}{f_o}\right) \quad (8)$$

Where PLoad.i and fi represent the load's active power consumption and the frequency of the PCC voltage after islanding, respectively. The DG operating at unity power factor does not generate

International Journal of Research
Available at https://edupediapublications.org/journals
e-ISSN: 2348-6848
p-ISSN: 2348-795X
Volume 04 Issue-17
December 2017

reactive power. According to (8), the needed reactive power disturbance to force the frequency to deviate from fi to its target value (Qdis) can be expressed as follows:

$$Q_{dis} = P_{DG} Q_f \left(\frac{f_o}{f_i + \Delta f} - \frac{f_{i+\Delta f}}{f_o} \right) \quad (9)$$

Where Δf represents the frequency deviation and it can be expressed as

$$\Delta f = f_{i.tar} - f_i \quad (10)$$

Where fi.tar represents the target frequency and it can be set at any value that is out of the frequency's normal range. For the DG operating at unity power factor, assuming that PDG is equal to 1, Fig. 3 illustrates the relationship between fi and Qdis with fi.tar being set at the threshold values.

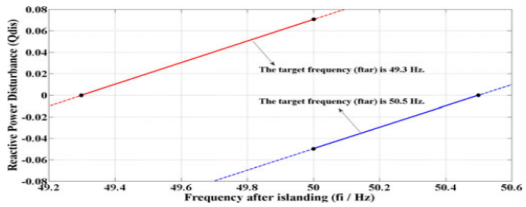

Fig. 3. Relationship between *fi* and *Q*dis for the DG operating at unity power factor.

However, the relationship between Qdis and Δf should be modified when the DG supplies both active and reactive power for the local load. If there are no power mismatches, the frequency will not change after islanding. According to (8), Qdis for the DG of this kind can be expressed as follows

$$Q_{dis} = P_{DG} Q_f \left(\frac{f_o}{f_{i.tar}} - \frac{f_{i.tar}}{f_o} \right) - P_{DG} Q_f \left(\frac{f_o}{f_i} - \frac{f_i}{f_o} \right)$$
$$= -P_{DG} Q_f \Delta f \left(\frac{f_o}{f_i (f_i + \Delta f)} + \frac{1}{f_o} \right) \quad (11)$$

Condition 1: Assuming that PDG is equal to 1 and f0 is equal to 50 Hz, Fig. 4 illustrates the relationship between fi and Qdis with fi.tar being set at the threshold values.

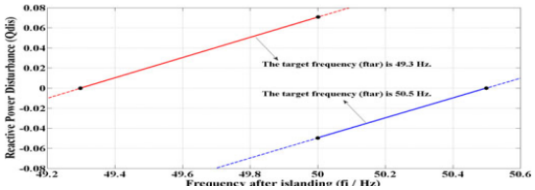

Fig. 4. Relationship between *fi* and *Q*dis for the DG generating both active and reactive power (*f*0 is set at 50 Hz).

Compared with Fig. 3, Fig. 4 shows approximately the same Qdis–fi curve. Condition 2: Assuming that PDG is equal to 1 and fi is equal to 50 Hz, Fig. 5 illustrates the relationship between f0 and Qdis with fi.tar being set at the threshold values. It can be seen from Fig. 5.

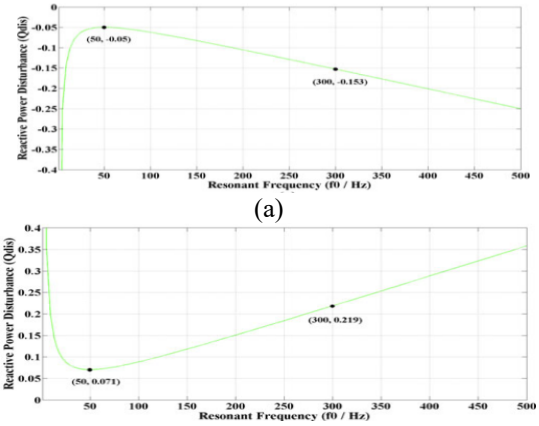

Fig. 5. Relationship between *f*0 and *Q*dis for the DG generating both active and reactive power (a) *fi* and *fi*tar are set at 50 Hz and 50.5 Hz, respectively (b) *fi* and *fi*tar are set at 50 Hz and 49.3 Hz, respectively.

Therefore, following two important conclusions can be obtained: 1) for the load whose resonant frequency f0 is actually unknown in advance, the calculated Qdis might be not sufficient enough to drive fi to deviate to fi.tar with f0 being set at 50 Hz in (11) and 2) for the same load, the frequency variation with f0 being set at 300 Hz is about three times as much as that with f0 being set at 50 Hz.

B. Islanding Detection Methods Proposed

Based on the RPV Owing to the smaller disturbance amplitude analyzed previously, islanding detection methods based on the reactive power disturbance might be better choices than those based on the active power disturbance.

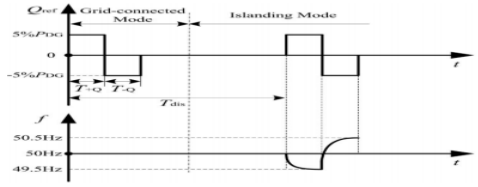

Fig. 6. *Q*ref and corresponding frequency in both operation modes with the method proposed

Fig. 6 illustrated Qref and corresponding frequency in both grid-connected and islanding modes, respectively.

According to, Qref for the DG in different frequency conditions was shown in Fig. 7. For the DG operating at unity power factor, the rated value of Qref is zero.

International Journal of Research
Available at https://edupediapublications.org/journals
e-ISSN: 2348-6848
p-ISSN: 2348-795X
Volume 04 Issue-17
December 2017

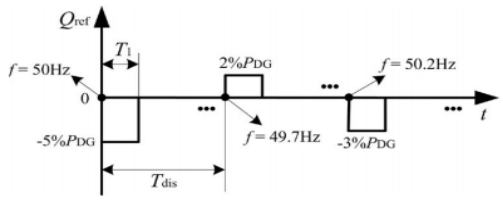

Fig. 7. Reactive power reference of the DG with different values of the frequency.

However, when they were applied to multiple DGs, the synchronization of the variations could not be guaranteed in both methods. Owing to the averaging effect, they might fail to detect islanding for the system with multiple DGs.

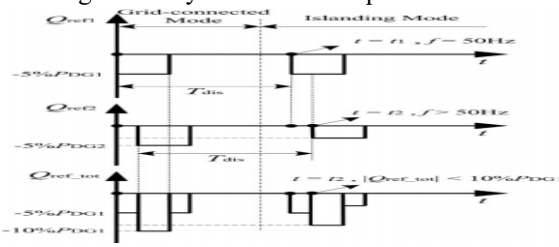

Fig. 8. Separate and total reactive power variations for the system with twoDGs according to the method

According to the method in Fig. 8 illustrated the separate and total reactive power variations for the system with two DGs, where the reactive power variation on the DG2 lagged behind that on the DG1 and f0 is 50 Hz. Therefore, when islanding occurred, the variation on the DG1 forced the frequency to increase earlier and the frequency was larger than 50 Hz when the variation on the DG2 started. Accordingly, the magnitude of the variation on the DG2 was less than 5%PDG2.

III. PROPOSED ISLANDING DETECTION METHOD BASED ON REACTIVE POWER DISTURBANCE

In order to improve the performance of islanding detection methods that are based on the reactive power disturbance, following three problems have to be solved: 1) the method has to be applicable for both the DG operating at unity power factor and that generating reactive power as well; 2) the disturbance on the DG is better to be reduced as much as possible during normal operation and it also has to be sufficient to drive the frequency outside its threshold limits after islanding; and 3) the synchronization of the disturbances on different DGs has to be guaranteed.

In addition, the design of the FSORPD also has to comply with following two principles: 1) reducing disturbance as much as possible during normal operation and 2) forming criterions for starting the SSORPD after islanding. In order to meet aforementioned requirements, the FSORPD is designed to contain two parts whose amplitudes are Qdis1 and 2Qdis1, respectively, and it is added on the DG's rated reactive power reference periodically. The value of Qdis1 is equal to either Qdis11 or Qdis12, which depends on the frequency at the beginning of the FSORPD. Fig. 9 illustrates the FSORPD with different values of f and corresponding frequency variation during islanding, respectively. The FSORPD causes the sudden mismatch of the reactive power during islanding and accordingly there is a transient response of the frequency.

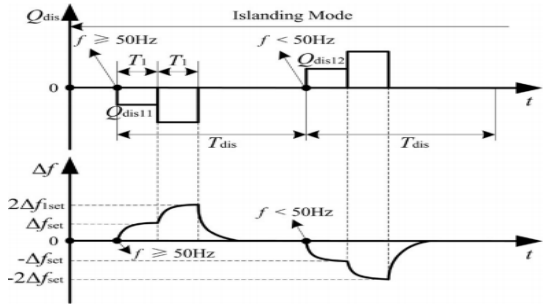

Fig. 9. FSORPD with different values of *f* and corresponding frequency variation during islanding.

There are two possible conditions that the FSORPDs are asynchronous: 1) the overlap region exists among the FSORPDs on several DGs and 2) the FSORPD on a certain DG does not overlap with the FSORPDs on the other DGs.

Moreover, the value of Twin has to be either equal to that of T1 or no more than that of (T1 − Ttra). Therefore, (16) is configured as the third criterion for disturbance switching. The aforementioned three criterions for switching the disturbance from the FSORPD to the SSORPD are shown in Table I.

TABLE I
CRITERIONS FORSWITCHING THEDISTURBANCEFROM THEFSORPDTO THESSORPD

criterion	content	Corresponding condition
First	1)f >50.3Hz or f<49.7Hz;2)its duration time is no less than T_{dur}	The FSORPDs are synchronous or the non synchronization is not serious
Second	1)the SOAFV is periodic ;2) its cycle time is equal to T_{dis}	1)The FSORPDs are asynchronous 2)some FSORPDs overlap with each other

International Journal of Research
Available at https://edupediapublications.org/journals
e-ISSN: 2348-6848
p-ISSN: 2348-795X
Volume 04 Issue-17
December 2017

Third	1)the SOAFV satisifies equation ;2) the frequency variation is not zero	1)The FSORPDs are asynchronous 2)a certain FSORPDs overlap with each other

TABLE II CRITERIONS FOR ISLANDING DETERMINATION

criterion	content	Suitable application
First	1)f >50.5Hz or f<49.3 Hz;2) its duration time is no less than T_{dur} .	1)the DG operating qt unity power factor ;2) the DG generating both active and reactive power
Second	1)the SOAFV satisfies equation ;2) the frequency variation is not zero	The DG generating both active and reactive power

The second and third criterions complement each other, which can reduce the starting time of the SSORPD. Moreover, these two criterions reflect the frequency variation characteristics corresponding to the frequency variation characteristics corresponding to the FSORPD during islanding.

In case of no islanding switching evens, which may transiently impose a significant frequency deviation as well, the duration time of above abnormal frequency condition has to be no less than Tdur to determine islanding.

TableIII
Time Variables and Their Meanings

Time Variable	Meaning
T_1	The duration time of each part in both the FSORPD and the SSORPD.
T_{dis}	The period time of the FSORPD.
T_{win}	The measurement window size for SOAFV calculation.
T_{tra}	The transient time of frequency deviation from a steady value to another steady one.
T_{dur}	The duration time of the abnormal frequency state.

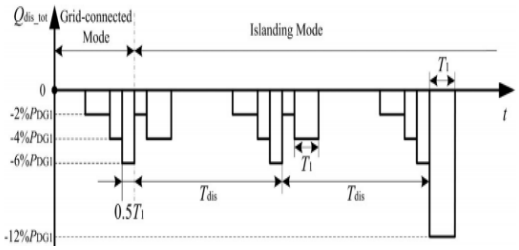

Fig. 10. Schematic diagram of the maximum islanding detection time.

Assuming that the active power references of two DGs are same (PDG1 = PDG2) and the FSORPD on the DG2 lags 1.5T1 behind that on the DG1, Fig. 10 illustrates the maximum detection time of the proposed method when islanding occurs.

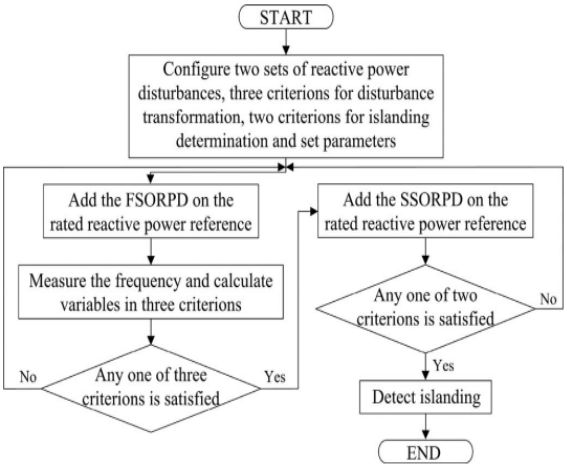

Fig. 11. Flowchart of the proposed islanding detection method

Generally, the FSORPD is added on the rated reactive power reference of the DG. If any of three criterions for disturbance switching is satisfied, the SSORPD will take the place of the FSORPD.

IV. PERFORMANCE OF THE PROPOSED ISLANDING DETECTION METHOD

In this section, several test cases are simulated on the power systems computer-aided design (PSCAD)/Electro magnetic transient in DC system (EMTDC) based on the system in Fig. 1.

A. Performance of the Proposed Method for the DG Operating at Unity Power Factor

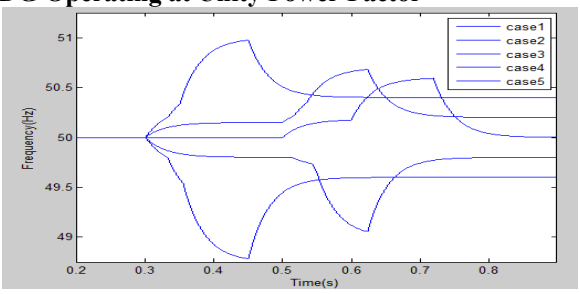

(a)

International Journal of Research
Available at https://edupediapublications.org/journals
e-ISSN: 2348-6848
p-ISSN: 2348-795X
Volume 04 Issue-17
December 2017

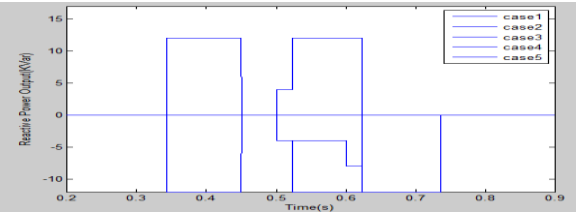

Fig. 12. Simulation results for loads with different values of *f*0 during islanding (a) The PCC frequency (b) The DG's reactive power output.

It can be noted from Fig. 12(a) that frequencies deviate outside the threshold limits in all five cases and islanding can be detected with different detection time.

Table IV
Simulation Results for Different Test Cases Part A

Case	f_o /Hz	Startup time of the SSORPD/ms	Detection result	Detection Time/ms
1	50	324	detected	356
2	50.2	226	detected	245
3	50.4	42	detected	60
4	49.8	224	detected	260
5	49.6	42	detected	70

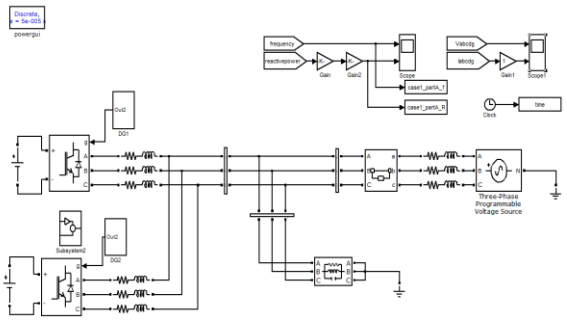

Fig.13 Block diagram of simulation

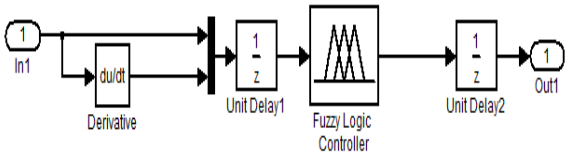

Fig.14 Block diagram of Fuzzy controller

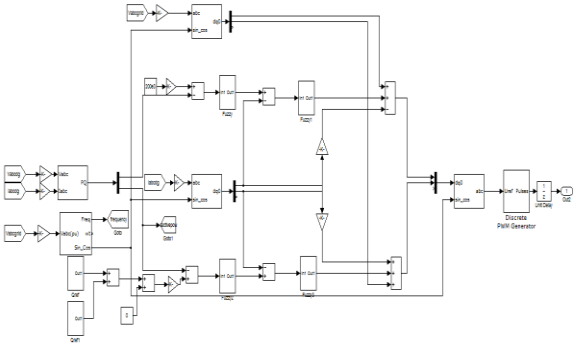

Fig.15 Control block diagram of simulation

III. FUZZY LOGIC CONTROLLER

In FLC, basic control action is determined by a set of linguistic rules. These rules are determined by the system. Since the numerical variables are converted into linguistic variables, mathematical modeling of the system is not required in FC.

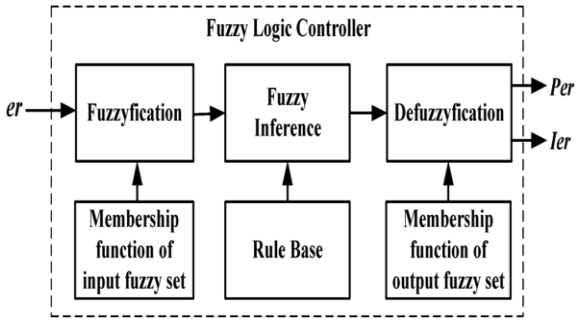

Fig.16.Fuzzy logic controller

The FLC comprises of three parts: fuzzification, interference engine and defuzzification. The FC is characterized as i. seven fuzzy sets for each input and output. ii. Triangular membership functions for simplicity. iii. Fuzzification using continuous universe of discourse. iv. Implication using Mamdani's, 'min' operator. v. Defuzzification using the height method.

TABLE III: Fuzzy Rules

e / $\dot{e}$	NB	NM	NS	ZE	PS	PM	PB
NB	NB	NB	NB	NB	NM	NS	ZE
NM	NB	NB	NB	NM	NS	ZE	PS
NS	NB	NB	NM	NS	ZE	PS	PM
ZE	NB	NM	NS	ZE	PS	PM	PB
PS	NM	NS	ZE	PS	PM	PB	PB
PM	NS	ZE	PS	PM	PB	PB	PB
PB	ZE	PS	PM	PB	PB	PB	PB

Fuzzification: Membership function values are assigned to the linguistic variables, using seven fuzzy subsets: NB (Negative Big), NM (Negative Medium), NS (Negative Small), ZE (Zero), PS (Positive Small),

International Journal of Research
Available at https://edupediapublications.org/journals
e-ISSN: 2348-6848
p-ISSN: 2348-795X
Volume 04 Issue-17
December 2017

PM (Positive Medium), and PB (Positive Big). The Partition of fuzzy subsets and the shape of membership CE(k) E(k) function adapt the shape up to appropriate system. The value of input error and change in error are normalized by an input scaling factor.In this system the input scaling factor has been designed such that input values are between -1 and +1. The triangular shape of the membership function of this arrangement presumes that for any particular E(k) input there is only one dominant fuzzy subset. The input error for the FLC is given as

$$E(k) = \frac{P_{ph(k)} - P_{ph(k-1)}}{V_{ph(k)} - V_{ph(k-1)}} \quad (12)$$

$$CE(k) = E(k) - E(k\text{-}1) \quad (13)$$

Inference Method: Several composition methods such as Max–Min and Max-Dot have been proposed in the literature. In this paper Min method is used. The output membership function of each rule is given by the minimum operator and maximum operator. Table 1 shows rule base of the FLC.

Defuzzification: As a plant usually requires a non-fuzzy value of control, a defuzzification stage is needed. To compute the output of the FLC, „height" method is used and the FLC output modifies the control output. Further, the output of FLC controls the switch in the inverter. To achieve this, the membership functions of FC are: error, change in error and output

The set of FC rules are derived from

$$u=-[\alpha E + (1-\alpha)*C] \quad (14)$$

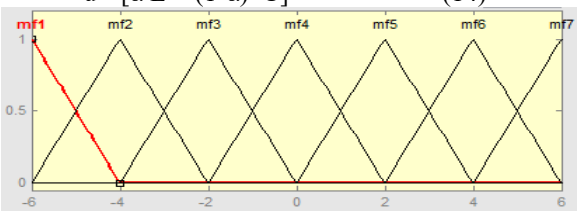

Fig 17 input error as membership functions

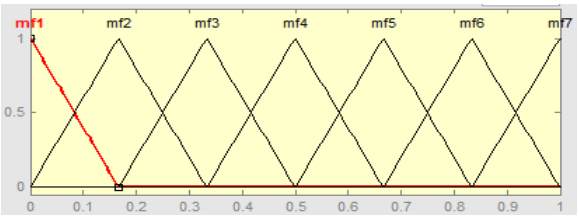

Fig 18 change as error membership functions

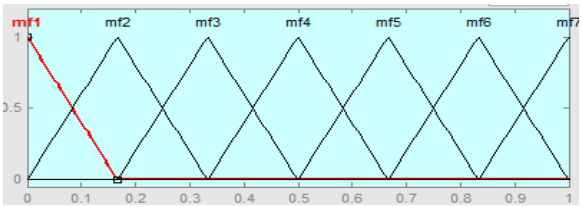

Fig.19 output variable Membership functions

Where α is self-adjustable factor which can regulate the whole operation. E is the error of the system, C is the change in error and u is the control variable.

Table VI
Load Parameter Setting For Different Test Cases in Part A

Case	R/Ω	L/mH	C/μF	f_0/Hz
1	0.8	1.0186	9947.2	50
2	0.8	1.0145	9907.6	50.2
3	0.8	1.0105	9868.2	50.4
4	0.8	1.0227	9987.1	49.8
5	0.8	1.0268	10027.4	49.6

It can be inferred from Fig. 20(a) that frequencies in all three cases eventually deviate outside the upper threshold 50.5 Hz and the duration time of this condition is longer than 10 ms. Moreover, it also can be seen from Fig. 20(a) that the fluctuation range of the PCC frequency is larger for the more unbalanced load.

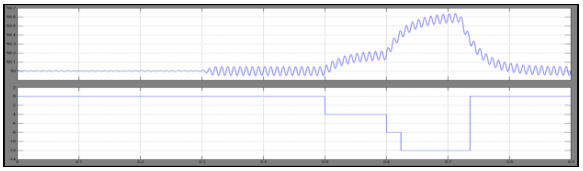

(a)

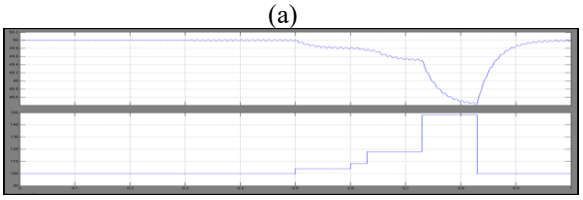

(b)

Fig. 20 Simulation results for unbalanced loads (a) The PCC frequency (b) The DG's reactive power output

B. Performance of the Proposed Method for the DG Generating Active and Reactive Power Simultaneously

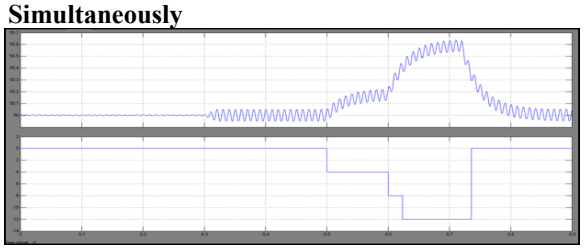

(a)

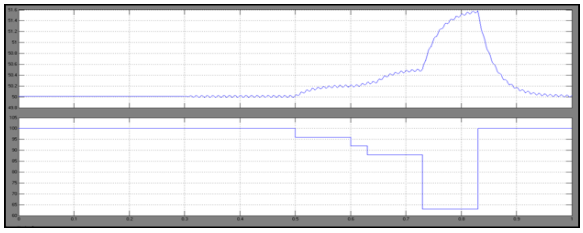

(b)

Fig. 21. Simulation results during islanding for the DG generating active and reactive power simultaneously (a) The PCC frequency (b) The DG's reactive power output.

Table VII
Load Parameter Setting For Different Test Cases In Part B

Case	R/Ω	L/mH	C/μF	f_e /Hz	ΔP so /kv	ΔQ s /kv
1	0.8	0.9218	9002.1	55.3	0	0
2	0.7619	0.9218	9002.1	55.3	10	0
3	0.8421	0.9218	9002.1	55.3	-10	0
4	0.8	0.9415	8930.7	5.7	0	8
5	0.8	0.9292	9074.1	54.8	0	-8

Fig. 21 illustrates the PCC frequency and the DG's reactive power output during islanding in each case of Part B. Accordingly, compared with the frequency in case 1, it can be seen from Fig. 21 (a) that the frequency starts to descend in case 2 or rise in case 3 once islanding occurs.

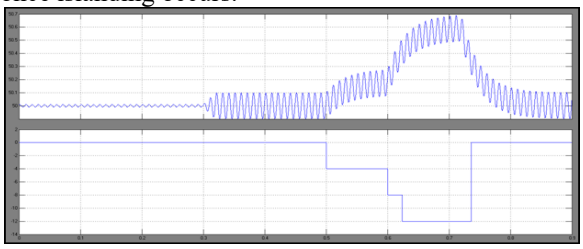

(a)

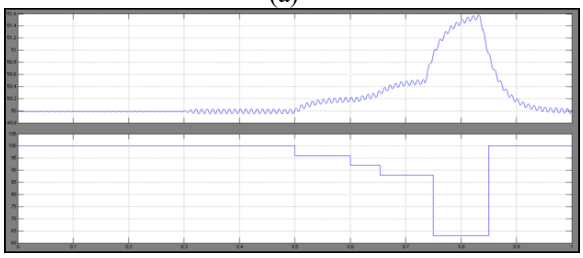

(b)

Fig. 22. Simulation results for unbalanced loads (a) The PCC frequency (b) The DG's reactive power output.

Fig.22 shows the simulation results in these three cases. It can be seen from Fig. 16(a) that frequencies in all three conditions deviate outside the threshold limits and the duration time of this condition is longer than 10 ms.

C.Comparison of the Performance of the Proposed Method with that of the Methods for the DG Operating at Unity Power Factor under Multiple-DG Operation Mode

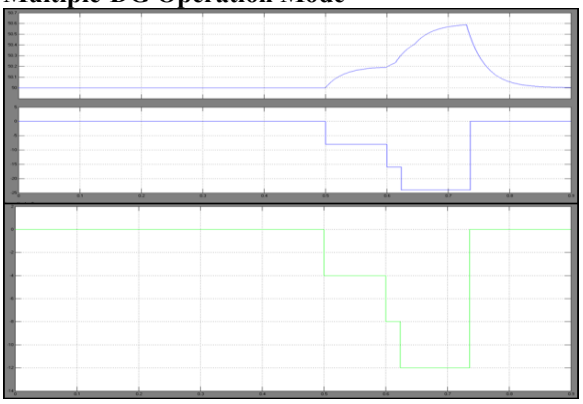

Fig. 23. Simulation results with three methods in scenario A (a) The PCC frequency (b) Separate reactive power output (c) The DG's total reactive power output.

For comparison, this situation is simulated as well in scenario B. Fig. 23 shows the PCC frequency and the DGs' total reactive power output in scenario A according to different methods. It can be seen from Fig. 22(a) that islanding can be detected with all these three methods in this scenario. Fig. 24 illustrates the simulation results in scenario B with the lag time equal to 80 ms.

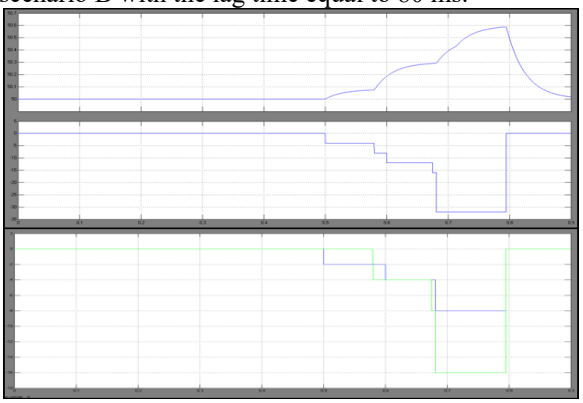

Fig. 24. Simulation results in scenario B (the lag time is 80 ms) (a) The PCC frequency (b) Separate reactive power output (c) The DG's total reactive power output.

However, it can be seen from Fig. 18 that the overlap part of the FSORPDs can still drive the frequency to be larger than 50.3 Hz with the method proposed in this paper, thus the SSORPDs are added on both DGs synchronously.

International Journal of Research
Available at https://edupediapublications.org/journals
e-ISSN: 2348-6848
p-ISSN: 2348-795X
Volume 04 Issue-17
December 2017

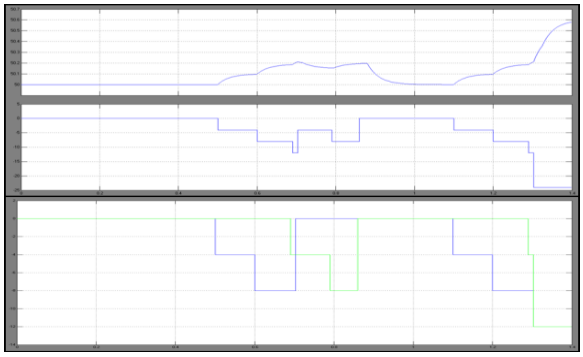

Fig. 25. Simulation results in scenario B (the lag time is 180 ms) (a) The PCC frequency (b) Separate reactive power output (c) The DG's total reactive power output

Fig. 25 illustrates the PCC frequency and the DGs' total reactive power output in scenario B with the lag time equal to 180 ms. as shown in Fig. 24, the maximum value of the frequency caused by this overlap part is 50.26 Hz, which is less than 50.3 Hz.

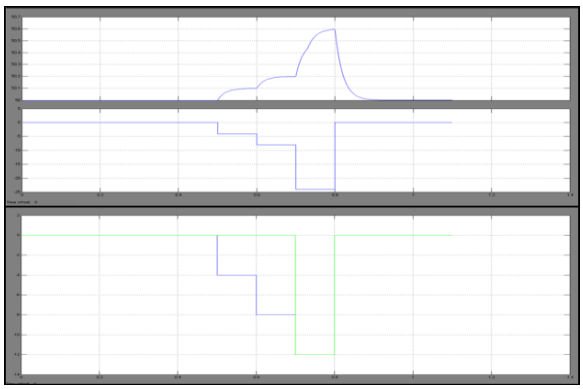

Fig. 26. Simulation results with three methods in scenario C (a) The PCC frequency (b) Separate reactive power output (c) The DG's total reactive power output.

CONCLUSION

In this paper steady power control, the midst of the consistent power control, the inverter based DG can produce the both responsive and dynamic power in the same time; consequently this paper may watch the association among the receptive power unsettling impact and the repeat in the amid of islanding. Fuzzy controller is meant as human basic decision making mechanism which gave the operation to the electronic system with the master choice. The proposed procedure may involve two courses of action of responsive power disrupting impacts. They moreover have the distinctive term time and size for various purposes. Furthermore the sizes of the FSORPD are less so which may lessen the impact on the structure in the amid of standard operation. In this way, DGs may be arranged at various positions which can recognize the equivalent repeat the comparable recurrence variety attributes operation mode is, which guarantees the synchronization of the SSORPDs on different DGs without the need of correspondence. Along these lines in like manner to the proposed system it can be reliably and reasonably recognize islanding for the diverse DG operation. Comparing with the PI controller the fuzzy controller eliminates the ripples, then total harmonic distortion also reduced. This paper is checking reproduction aftereffect of the proposed technique by utilizing the tangle lab/simulink.

REFERENCES

[1] H. B. Puttgen, P. R. MacGregor, and F. C. Lambert, "Distributed generation: Semantic hype or the dawn of a new era?," IEEE Power Energy Mag., vol. 1, no. 1, pp. 22–29, Jan./Feb. 2003.

[2] P. P. Barker and R. W. de Mello, "Determining the impact of distributed generation on power systems: Part 1—Radial distribution systems," in Proc. IEEE Power Eng. Soc. Summer Meeting, Jul. 2000, pp. 1645–1656.

[3] IEEE Recommended Practice for Utility Interface of Photovoltaic (PV) Systems, IEEE Standard 929-2000, Apr. 2000.

[4] IEEE Standard for Interconnecting Distributed Resources with Electric Power Systems, IEEE Standard 1547-2003, Jul. 2003.

[5] R. A. Walling and N. W. Miller, "Distributed generation islanding— Implications on power system dynamic performance," in Proc. IEEE Power Eng. Soc. Summer Meeting, Jul. 2002, pp. 92–96.

[6] G. Hernandez-Gonzalez and R. Iravani, "Current injection for active islanding detection of electronically-interfaced distributed resources," IEEE Trans. Power Del., vol. 21, no.3, pp. 1698–1705, Jul. 2006.

[7] A. Timbus, A. Oudalov, and N. M. Ho Carl, "Islanding detection in smart grids," in Proc. IEEE Energy Convers. Congr. Expo., Sep. 2010, pp. 3631– 3637.

[8] D. Reigosa, F. Briz, C. Blanco, P. Garcia, and J. M. Guerrero, "Active islanding detection for multiple parallel-connected inverter-based distributed generators using high-frequency signal injection," IEEE Trans. Power Electron., vol. 29, no. 3, pp. 1192–1199, Mar. 2014.

[9] F. De Mango, M. Liserre, A. D. Aquila, and A. Pigazo, "Overview of antiislanding algorithms for PV systems. Part I: Passive methods," in Proc. IEEE

Power Electron. Motion Control Conf., Aug. 2006, pp. 1878–1883.

MD.ATHER ALI

Completed B.E in Electrical & Electronics Engineering in 2015 from JNTU UNIVERSITY, HYDERABAD and Pursuing M.Tech form B.V.Raju Institute of Technology, Narsapur, Telangana, India. Area of interest includes Power Electronics.

E-mail id;mohammad.ather93@gmail.com

KOTHURI RAMAKRISHNA

completed his Bachelor of Engineering (B.E.)in Department of EEE from Gulbarga University in the year 1998 and Master of Technology (M.Tech.)in Power Engineering from J.N.T.U Hyderabad in 2001. He also completed Master of Business Administration (MBA) in HR from Annamalai University in 2013. Presently, he is pursuing Ph.D from J.N.T.U. Hyderabad Telangana, India.He has around 19 years of teaching experience. He is working as Associate professor in B. V. Raju Institute of Technology, Narsapur, Medak district of Telangana from 2008. He worked as Associate Professor in Vardhamaan Engineering College from 2005 to 2008. He worked as Assistant Professor in Adams Engineering College Palvancha, Khammam District of Telangana 1998 to 2005.In His research interest includes, Electrical Distribution Systems, Power System Analysis. He has published several National and International Journals and Conferences. He have Professional Society memberships in IEEE (M), IETE (M), ISTE (LM),FIE (AM), SESI (LM), IAENG (M), NIQR (M), SSI (LM), SPE (LM), IAENG (LM), IACSIT (LM), and C.Eng.Presently he is counselor of IEEE student branch,co counselor for PEES(IEEE)of BVRIT,Narsapur,Medak district telangana.